Journal of Thermal Analysis and Calorimetry, Vol. 75 (2004) 947–956

THERMAL ANALYSIS OF LOW ALLOY Cr–Mo STEEL

M. Gojić[1]*, *M. Sućeska*[2] *and M. Rajić*[2]

[1]Faculty of Metallurgy, University of Zagreb, Aleja narodnih heroja 3, Sisak, Croatia
[2]Shipbuilding Institute and Special Technology, Laboratory for Thermal Analysis,
Avenija V. Holjevca 20, 10000, Zagreb, Croatia

(Received April 5, 2003; in revised form September 20, 2003)

Abstract

The paper deals with results of thermal analysis of low-alloyed chromium–molybdenum steel. The methods of analysis were dilatometry, differential thermal analysis (DTA) and differential scanning calorimetry (DSC). The Ac_1 and Ac_3 temperatures of the steel samples measured by dilatometry and DTA during the heating period were in good agreement. Generated by cooling a martensitic structure first became apparent at 503 K. Tempering of the as-quenched samples showed the presence of the second tempering stage in the region between 473 and 573 K. At that stage heat capacity decreased from 0.48 to 0.32 J g^{-1} K^{-1}, as a result of conversion of transition carbide due to heat consumption. After normalization of the as-quenched samples the heat capacity values were restored to between 0.42 and 0.47 J g^{-1} K^{-1} in the temperature range from 373 to 673 K.

Keywords: low-alloyed steel, microstructure, specific heat, tempering, thermal analysis

Introduction

Transformation kinetics of low alloy steels is rather complex. The austenite-to-martensite phase transformation depends on the chemical composition of steel, the austenite microstructure preceeding transformation, and the cooling rate [1]. The microstructure as a result of transformation will depend on the combined effect of all those factors.

The methods most commonly used for determining structural transformations of low alloy steel in terms of thermal cycling are dilatometry and thermal analysis [2–6]. Dilatometry provides information on the consequences of transformations by the study of changes in the sample length, which occur when phase changes are involved. When steel undergoes a phase change, the lattice structure becomes altered and, as a rule, produces a change in specific volume. Differential thermal analysis (DTA) and differential scanning calorimetry (DSC) are frequently applied to study the reaction and transformation kinetics of steel. DTA is [7, 8] a technique in which

---

* Author for correspondence: E-mail: gojic@siscia.simet.hr

1388–6150/2004/ $ 20.00

Akadémiai Kiadó, Budapest
Kluwer Academic Publishers, Dordrecht

the difference in temperature between the sample and a reference material is monitored *vs.* time or temperature. DSC is a technique in which the difference in heat flow to the sample and a reference is monitored *vs.* time or temperature.

Iron-carbon martensite can be described as a body-centered tetragonal lattice of iron atoms. The carbon atoms are randomly distributed over the *c*-type octahedral interstices [9]. From the thermodynamic point of view, tempering is an irreversible process, in the course of which a system reaches a more stable, stationary state. During the treating of quenched steel up to the tempering temperature there are gradients in the chemical potentials of carbon, chromium and molybdenum with respect to carbide phases and the solid solution. Although significant advances have been made in identifying the processes accompanying the tempering, a complete and satisfactory understanding of the mechanisms of the structural changes involved has not yet been reached [10–12]. A comprehensive study using dilatometry, DTA and DSC, likewise, has not been undertaken. Combined use of dilatometry and calorimetry could be particularly rewarding, as tempering processes are likely to be accompanied by heat production and a small change in sample length.

This work deals with the results of dilatometry, DTA and DSC of low alloy chromium–molybdenum steel during the period of quenching and tempering.

Experimental

Longitudinally-oriented test samples, 2 mm in diameter and 12 mm long, were machined from the pipes size ∅57×4.83 mm. Tests were carried out using the heating system of a LK02 Adamel Lhomargy dilatometer.

The sample was mounted between a quartz probe connected to a linear variable differential transformer (LVDT) and a quartz support tube. It was kept in a vacuum at all testing times to minimize oxidation and decarburization of the outer surfaces. The temperature of the sample was measured with chromel–alumel thermocouples spot welded to its outer surface.

Dimensional changes were recorded by means of a LVDT placed in a sealed chamber. A carrier current measurement system transformed the displacement applied to the LVDT core into a voltage which was proportional to the displacement. The voltage was then transmitted to the recorder. The sample expansion or contraction was recorded as a function of temperature on the flat recorder.

The furnace temperature, the heating rate, and the plateau temperature and duration were programmed. The samples were heated to 1123 K, at a rate of 2 K s^{-1}. They were kept at the austenitizing temperature for 1200 s. Quenching was performed by blowing argon through a perforated tube into the sealed chamber and over the entire sample surface. Argon was selected because of its high thermal conductivity. Tempering of the samples was carried out at 823 K for 3600 s.

Thermal analysis of the steel samples was performed by means of a differential thermal analyser (TA Instruments SDT Model 2960) and a differential scanning calorimeter (DSC Model 2910). The samples with a mass of about 30 mg (discs with a diameter of 2 mm and a height of 4 mm) were annealed in an open platinum pan. Nitrogen was used to provide a protective atmosphere (flow rate 1.6 mL s^{-1}). The temperature and power axes of the instrument were calibrated by means of indium. Heating was conducted continuously, at a rate of 0.08 K s^{-1}, from room temperature to 823 K for DSC, and to 1173 K for DTA.

Table 1 Chemical composition of low alloy Cr–Mo steel, mass%

C	Si	Mn	P	S	Cr	Mo
0.40	0.33	0.85	0.014	0.0124	1.02	0.24

Determination of heat capacity by the DSC method was carried out in three stages. The first stage comprised isothermal stabilization of samples at 30 K for 600 s. The second stage included dynamic measurements up to 823 K, at a heating rate of 0.16 K s^{-1}. After that the samples were isothermally stabilized at the temperature of 823 K for 600 s. During DSC measurements Al_2O_3 was used as standard. The baseline was determined by reheating the unfilled pan.

Metallographic examination of the samples was performed with a Jeol JXA-50A scanning electron microscope. Nital solution was used to reveal the microstructure. Hardness was measured by the Vickers method (HV_{30}).

Results and discussion

Low alloy Cr–Mo steel, after hot rolling, showed a bainitic microstructure (Fig. 1) with a hardness of 380 HV_{30} (Table 2). Classic bainite is a non-lamellar mixture of ferrite and carbide generally regarded as an aggregate of ferrite and residual phases, such as retained austenite, carbide or martensite [13]. Figure 1 shows carbide particles in the ferrite matrix.

Table 2 Hardness of low alloy Cr–Mo steel for different states

State of steel	Hardness, HV_{30}
Hot rolled	380
As-quenched	685
Quenched and tempered	348

The length changes recorded for the low alloy Cr–Mo steel samples during the heating and cooling periods are shown in Fig. 2. It is seen in the curves that during continuous heating from room temperature to Ac_1, normal thermal expansion of the sample took place. The Ac_1–Ac_3 segment implies the occurrence of $\alpha \rightarrow \gamma$ transformation which led to length contraction as a result of austenite formation. The experiment also allowed direct measurement of the martensite start temperature (M_S) during cooling from the austenitic state at a rate of 30 K s^{-1}. An average cooling rate was calculated according to the Eq. [14]:

Fig. 1 SEM micrograph of low alloy Cr–Mo steel after hot rolling. Arrows point to carbide particles

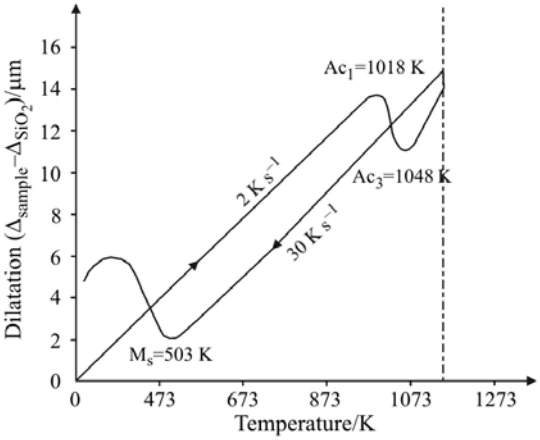

Fig. 2 Dilatometric curves of low alloy Cr–Mo steel after heating and after cooling with argon; heating rate 2 K s^{-1}, cooling rate 30 K s^{-1}

$$V_c=\frac{T_A-T_i}{t_2-t_1} \tag{1}$$

where T_A is the austenitization temperature (1123 K), T_i is the assumed temperature for calculation (773 K), t_1 is the time of initiation of cooling (t_1=0), t_2 is the time when the sample cooled to 773 K.

Upon cooling of low alloy Cr–Mo steel from 1123 to 773 K, at the rate of 30 K s^{-1}, the austenite having a face-centered cubic structure transformed, at 503 K, into the martensite having a tetragonal structure (Fig. 2). Figure 3 shows a typical ‘zig-zag’ patchwork of martensite laths. Martensite forms by a shear mechanism where many atoms move cooperatively and almost simultaneously in contrast to atom-to-atom movements during diffusion-controlled transformations. In the investigated steel, the predominant lattice deformation mechanism was a slip and, accordingly, the microstructure was composed of lath martensite [15]. It was a hard and brittle structure. The hardness of the steel in the quenched state was 685 HV_{30}. Identical martensitic structure was first examined by Vetters by means of transmission electron microscopy [16]. It consisted of interconnected laths with a high dislocation density. The laths were of about 10 μm.

In general, the martensitic microstructure needs to be tempered to yield an optimum combination of strength and toughness. The tempering process usually produces a decrease in strength due to the precipitation of iron carbides from the carbon that is originally present in solid solution in the martensite. Tempering must be carried out at a temperature below that of Ac_1 because partial austenite formation during tempering would lead to the formation of brittle untempered martensite on cooling.

Figure 4 shows a typical ferrite–carbide microstructure after tempering at 823 K. The martensite recovery during tempering is clearly visible. The transition from the quenched state (Fig. 3) to the tempered state (Fig. 4) was accompanied by a break-up of the martensite laths as well as by precipitation and spheroidization of carbides. The precipitation of the cementite was probably present. It was confirmed by the hardness of 348 HV_{30} (Table 2).

Fig. 3 SEM micrograph of low alloy Cr–Mo steel after quenching at a rate of 30 K s^{-1}. Arrows point to martensite laths

Fig. 4 SEM micrograph of low alloy Cr–Mo steel after tempering at 823 K for 360 s. Arrows point to carbide particles

Figure 5 shows the DTA curves at the heating rate of 0.08 K s^{-1} with the onset points labelled Ac_1 and Ac_3. The endothermic peak appears between Ac_1 and Ac_3. The onsest point indicates the beginning of austenite formation and the second marks its end. There is a good agreement between the Ac_1 and Ac_3 temperatures determined by dilatometry (Fig. 2) and those shown by DTA curves (Fig. 5). The transformation behaviour of low alloy Cr–Mo steel in the hot-rolled state was quite different from that in the as-quenched state (Fig. 5). Comparison of DTA curves showed the steel to have a peak at 893 K following quenching. The peak was most likely related to the tempering process. Further studies will be performed to clarify its origin. This behaviour is similar to the one reported by Rodríguez *et al*. [17] who studied the kinetics of the recovery and recrystallization of cold-rolled steel. The Curie temperature (T_C) is not observable in Fig. 5. Its accepted value was approximately 1043 K [4]. The Curie temperature value partly overlapped with the peak corresponding to austenite formation. This was due to the fact that the two effects occurred simultaneously [18].

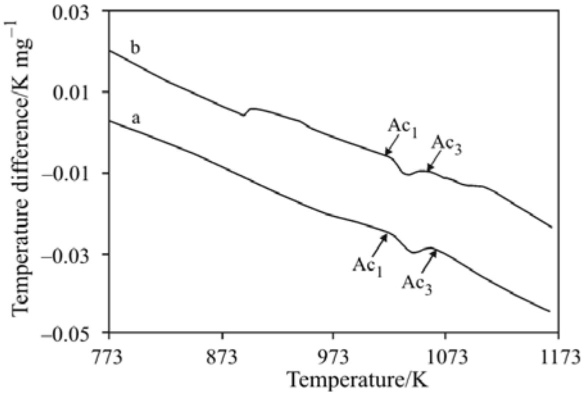

Fig. 5 DTA curves of low alloy Cr–Mo steel a – after hot rolling and b – after quenching at a rate of 30 K s^{-1}

Martensite tempering has been subject of numerous investigations involving low alloy steels. Previous studies indicate that the structural changes taking place during tempering can be grouped by three stages [19]. The first stage takes place at temperature around 373 K, the second close to 553 K and the third in the region of 553–803 K [20]. During the heating of samples up to 823 K, a decrease in relative length occurred between 573 and 673 K (Fig. 6). The decrease can be associated with the start of conversion of transition carbide into cementite. The formation of cementite at the expense of transition carbide leads to a decrease in the specific volume of the sample [21]. For low alloy Cr–Mo steel the first tempering stage was not observed. The second stage occurred between 473 and 573 K (Fig. 7). After quenching the samples were kept at 1173 K for 1200 s and then cooled in air. After this treatment the second tempering stage was not observed. A number of processes involving structural changes are known to occur in the temperature range between 473 and 573 K, for example, conversion of the transition carbide, decomposition of the

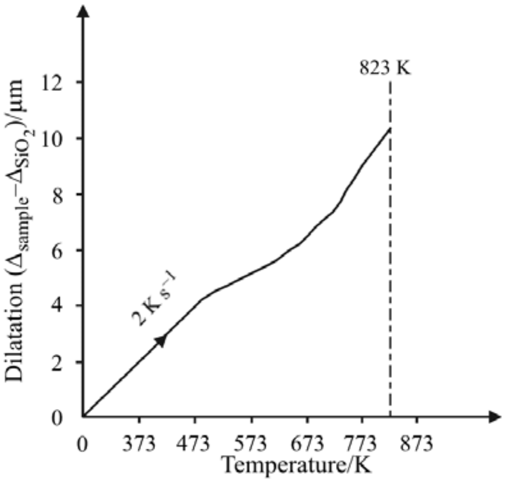

Fig. 6 Dilatometric curve of low alloy Cr–Mo steel during tempering; heating rate 2 K s^{-1}

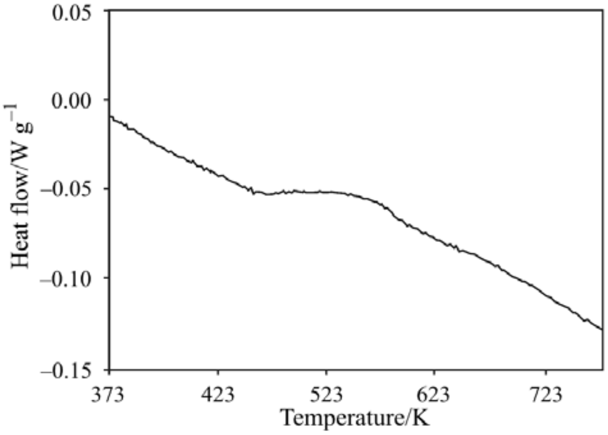

Fig. 7 DSC curve of low alloy Cr–Mo steel after quenching

retained austenite into ferrite, etc. These processes largely overlap. Figure 8 shows results of DSC measurements of the heat capacity of the steel quenched in a flow of argon. Heat capacity (C_p) was calculated using the equation:

$$C_p = \frac{K\Delta y}{dT/dt} \quad (2)$$

where K is the calorimeter sensitivity during calibration of equipment, Δy is the difference from the baseline to the sample line, and dT/dt is the heating rate (0.08 K s^{-1}).

Table 3 Specific heat of low alloy Cr–Mo steel for different states in the 373–673 K temperature range

State of steel	Temperature/K	Heat capacity/J g^{-1} K^{-1}
Hot rolled	373	0.31
	473	0.27
	573	0.28
	673	0.28
As-quenched	373	0.52
	473	0.50
	573	0.33
	673	0.42
Quenched and tempered	373	0.42
	473	0.43
	573	0.43
	673	0.47

In the temperature range of the second tempering stage heat capacity decreased from 0.52 to 0.32 J g^{-1} K^{-1} (Table 3). The C_p decrease determined by DSC measurements of the as-quenched sample between 473 and 573 K (Fig. 8) partly coincided with the decrease in relative length recorded by dilatometry (Fig. 6). It was therefore concluded that a drop in heat capacity was associated with the second tempering stage, and also, that the conversion of transition carbide was connected with the heat consumption. This was confirmed by the DSC curves for hot-rolled steel samples and for as-quenched samples normalized at 1173 K (Fig. 9). In these cases the heat capacity values were approximately constant in the temperature range from 373 to 673 K (Table 3).

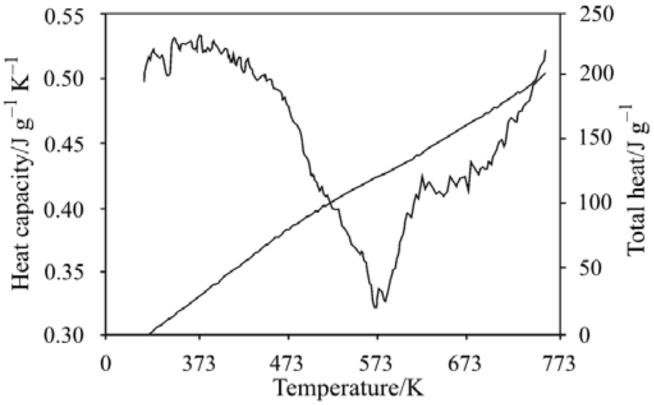

Fig. 8 Relationship of heat capacity and temperature for low alloy Cr–Mo steel after quenching

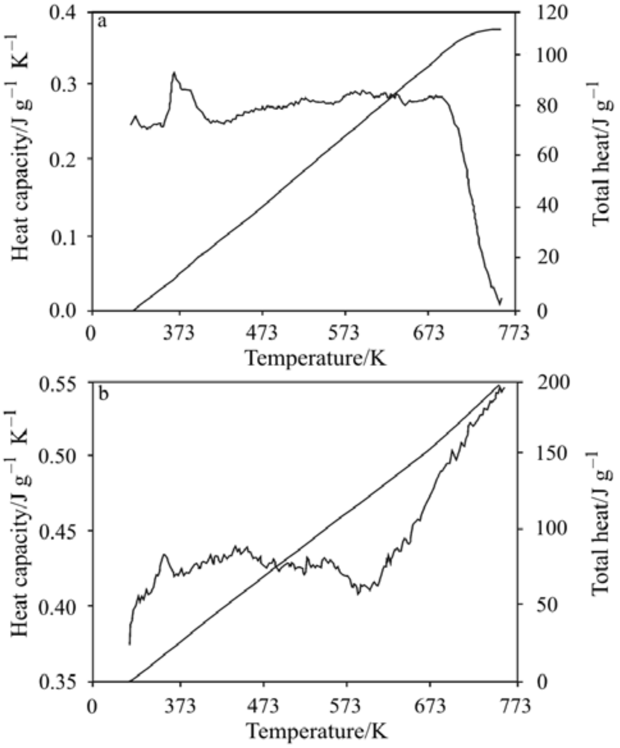

Fig. 9 Relationship of heat capacity and temperature for low alloy Cr–Mo steel a – after hot rolling and b – after normalization at 1173 K

Conclusions

After hot rolling, steel exhibited a bainitic microstructure with a hardness of 380 HV_{30}. Quenching in a flow of argon, at a rate of 30 K s^{-1}, yielded a martensitic microstructure at 503 K, with a hardness of 685 HV_{30}. During the tempering of the as-quenched sample from the room temperature to 823 K a break-up of the martensite laths as well as precipitation of carbides occurred. The results of dilatometry and differential thermal analysis showed that the second tempering stage occurred between 473 and 573 K. At that stage the conversion of transition carbides and decomposition of retained austenite into ferrite are likely to have taken place. This was confirmed by the results of DSC measurements. In the temperature range of the second tempering stage there was a decrease in heat capacity from 0.52 to 0.32 J g^{-1} K^{-1}. After normalization of the same samples at 1173 K heat capacity was approximately constant (0.42–0.47 J g^{-1} K^{-1}) in the region between 373 and 673 K.

References

1 P. V. Morra, A. J. Böttger and E. J. Mittemeijer, J. Therm. Anal. Cal., 64 (2001) 905.
2 M. Muscalu and D. Fatu, J. Therm. Anal. Cal., 52 (1998) 425.
3 A. Bodin and P. D. Marchal, Steel Research, 65 (1994) 103.
4 G. P. Krielaart, C. M. Brakman and S. Van der Zwaag, J. Mat. Sci., 31 (1996) 1501.
5 C. Qiu and S. Van der Zwaag, Steel Res., 68 (1997) 32.
6 M. Gojić, J. Črnko, M. Sućeska and M. Rajić, J. Therm. Anal. Cal., 62 (2000) 703.
7 R. Turcote, R. C. Fouchard, A.–M. Turcote and D. E. G. Jones, J. Therm. Anal. Cal., 73 (2003) 105.
8 J. P. Sandres and P. K. Gallagher, J. Therm. Anal. Cal., 72 (2003) 777.
9 M. J. Van Genderen, A. Böttgar, R. J. Cernik and E. J. Mittemeijer, Metallurgical Transactions, 24A (1993) 1965.
10 I. Pektas and H. Atila, J. Therm. Anal. Cal., 54 (1998) 803.
11 Y. Ichiyanagi and Y. Kimishima, J. Therm. Anal. Cal., 69 (2002) 919.
12 M. J. Van Genderen, A. Böttger, R. J. Cernik and E. J. Mittemeijer, Metallurgical Transactions, 24A (1993) 1965.
13 M. Hillert, ISIJ International, 35 (1995) 1134.
14 M. Gojić and R. Križanić, Strojarstvo, 36 (1994) 183.
15 R. Kaspar, U. Lotter and C. Biegus, Steel Research, 65 (1994) 242.
16 H. Vetters, Steel Research, 67 (1996) 408.
17 C. E. Rodríguez Torres, F. H. Sánchez, A. González, F. Actis and R. Herrera, Metallurgical and Materials Transactions, 33A (2002) 25.
18 A. Bodin and P. D. Marchal, Steel Res., 65 (1994) 103.
19 L. Cheng, C. M. Brakman, B. M. Korevaar and E. J. Mittemeijer, Metallurgical Transactions, 19A (1988) 2415.
20 S. Nagakura, Y. Hirotsu, M. Kusunoki, T. Suzuki and Y. Nakamura, Metallurgical Transactions, 14A (1983) 1025.
21 E. J. Mittemeijer, L. Cheng, P. J. Van der Schaaf, C. M. Brakman and B. M. Korevaar, Metallurgical Transactions, 19A (1988) 925.